Science of the Total Environment 700 (2020) 134432

Contents lists available at ScienceDirect

Science of the Total Environment

journal homepage: www.elsevier.com/locate/scitotenv

Dissolved organic matter in the deep TALDICE ice core: A nano-UPLC-nano-ESI-HRMS method

Roberta Zangrando [a,*], Veronica Zanella [b], Ornela Karroca [b], Elena Barbaro [a], Natalie M. Kehrwald [c], Dario Battistel [b], Elisa Morabito [b], Andrea Gambaro [a,b], Carlo Barbante [a,b]

[a] Institute of Polar Sciences CNR, Via Torino 155, 30172 Mestre (VE), Italy
[b] Department of Environmental Sciences, Informatics and Statistics, Ca' Foscari University of Venice, Via Torino 155, 30170 Mestre, VE, Italy
[c] U.S. Geological Survey, Geosciences and Environmental Change Science Center, Denver Federal Center, MS 980, Denver, CO 80225, USA

HIGHLIGHTS

- Untargeted characterization of samples from an Antarctic deep ice core.
- Four μL of ice were analyzed without preconcentration using nano-UPLC-nano-ESI-HRMS.
- Major species found were from fatty acids, isoprene and monoterpenes.
- Main sources of DOM were microbes as well as primary and secondary aerosols.
- Samples from glacial periods were less diverse species than those from interglacials.

GRAPHICAL ABSTRACT

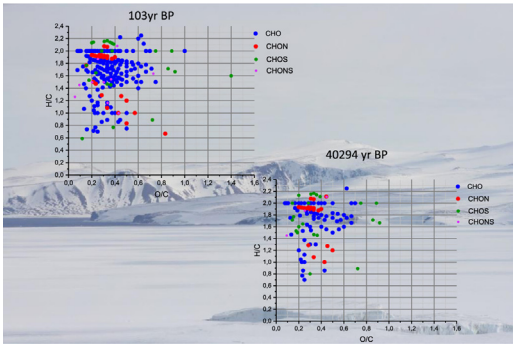

ARTICLE INFO

Article history:
Received 2 August 2019
Received in revised form 11 September 2019
Accepted 11 September 2019
Available online 13 September 2019

Editor: Dr. Damia Barcelo

Keywords:
Untargeted analysis
Ice cores
Nano-UPLC-nano-ESI-HRMS
Antarctica
TALDICE

ABSTRACT

Trace organic compounds in deep ice cores supply important paleoclimatic information. Untargeted analyses of dissolved organic matter provide an overview of molecular species in ice samples however, sample volumes usually required for these analyses are generally not available from deep ice cores. Here, we developed an analytical method using a nano-UPLC-nano-ESI-HRMS to detect major molecular species in ice cores. Samples (4 μL) from the TALos Dome Ice CorE (TALDICE), allowed investigating molecular species across a range of depths including during glacial and interglacial periods. We detected 317 chemical species that were tentatively assigned to fatty acids, hydroxy fatty acids and their degradation products (oxo-fatty acids and dicarboxylic acids), as well as oxidation byproducts of isoprene and monoterpenes. These compounds indicate that the main sources of the organic fraction are microbes as well as primary and secondary aerosols. Interglacial samples encompass a wide range of species including compounds from the oxidation of isoprene and monoterpenes as well as unsaturated fatty acids, while the glacial samples contained less diverse species. This difference may be due to decreased temperatures during the glacial period inhibiting terrestrial vegetation growth and increasing the sea ice extent, thereby weakening the emission sources.

1. Introduction

Deep polar ice cores supply reference records commonly used to correlate past hemispheric with global climate events (Veres

* Corresponding author.
E-mail address: roberta.zangrando@cnr.it (R. Zangrando).

https://doi.org/10.1016/j.scitotenv.2019.134432
0048-9697/

et al., 2013). These cores archive paleoclimatic and paleoenvironmental conditions through multiple glacial-interglacial cycles (Bradley, 2015; Wolff et al., 2010). Detailed physical and chemical analyses of ice and firn (Bradley, 2015) provide information on temperature, greenhouse gas concentrations in the atmosphere, sea ice extent, aerosol load, and biological productivity of the ocean (Wolff et al., 2010). Trace chemicals trapped in surface snow, and then compressed into glacial ice, can reveal a combination of changes in source strength, transport, deposition and preservation of aerosols reaching the ice core locations (Wolff et al., 2010). Dissolved organic matter (DOM) represents an important and complex component of polar snow and ice. DOM is composed of organic molecules of biological origin, which are deposited from aerosols (marine aerosols, vascular plant material, as well as combustion of fossil fuel and vegetal biomass) deposited from atmospheric gasses, or chemically produced *in situ* (Antony et al., 2014; Antony et al., 2017; Grannas et al., 2006; McNeill et al., 2012).

Understanding DOM at a molecular level can supply important clues regarding sources influencing chemical composition and/or post-depositional processes in the snowpack and ice. Although investigating the chemical composition of DOM in glacier ice is relatively new, similar investigations of other environmental matrices include natural waters (sea, river, lake) (Koch et al., 2005; Minor et al., 2012; Schmitt-Kopplin et al., 2012; Stubbins et al., 2010), atmospheric particulate matter (Kourtchev et al., 2013; Kourtchev et al., 2014b; Mazzoleni et al., 2012; Schmitt-Kopplin et al., 2012; Wozniak et al., 2008), clouds (Zhao et al., 2013), fog (LeClair et al., 2012; Mazzoleni et al., 2010) and rain (Altieri et al., 2009). In general, the organic fraction of the matrices is determined through the direct injection of samples using ultrahigh ($R \geq 100{,}000$) and high ($R \geq 60{,}000$) resolution mass spectrometry (UHRMS and HRMS) with ElectroSpray Ionization Fourier transform ion cyclotron resonance mass spectrometry (ESI FT-ICR-MS) (Mazzoleni et al., 2012; Wozniak et al., 2008; Zhao et al., 2013) and ESI-Orbitrap-MS (Kourtchev et al., 2013; Kourtchev et al., 2014a; Kourtchev et al., 2016; Kourtchev et al., 2014b; Laskin et al., 2009; Smith et al., 2009). Only a few studies apply LC/ESI-HRMS in order to identify the organic compounds (Kourtchev et al., 2015; Kourtchev et al., 2013; Kourtchev et al., 2014b). Detection limits are improved by pre-concentrating aqueous samples such as snow and fog (Antony et al., 2014; Antony et al., 2017; Grannas et al., 2006; LeClair et al., 2012; Mazzoleni et al., 2010), as well as the organic fraction in particulate matter after filter extraction (Mazzoleni et al., 2012; Zhao et al., 2013) through Solid-phase extraction (SPE).

Due to the very low concentrations (ranging from $\mu g\ L^{-1}$ to $ng\ L^{-1}$) (Barbaro et al., 2017; Giorio et al., 2018) of organic compounds in polar snow and ice, comprehensively characterizing DOM is a challenging task that requires pre-concentrating samples on SPE cartridges or disks from initial large volumes of samples that range between hundreds of mL to liters of melted ice or snow (Antony et al., 2014; Antony et al., 2017; Bhatia et al., 2010; Grannas et al., 2006). These large melted ice volume amounts are generally also required to determine biomarkers in snow and ice (Giorio et al., 2018). This approach is feasible when using shallow cores that are specifically drilled to provide large sample volumes for biomarker or organic compound analysis. However, deep ice cores, spanning hundreds of thousands of years, are designated for multi-proxy records where only a few milliliters are available for each analysis.

Investigating DOM in deep ice cores with sub-mL sample sizes requires an analytical technique with an extremely high sensitivity. Previous applications of nano-UPLC-nano-ESI-HRMS techniques, such as in investigating proteomics, provide valuable results where a limited amount of sample was available (Shen et al., 2002). Here, we evaluate the possibility of applying nano-UHPLC-nano-ESI-HRMS to polar ice samples for untargeted compound analysis, while using only a few μL of melted ice. We tested the nano-UPLC-nano-ESI-HRMS method with six ice samples from the coastal Antarctic TALos Dome Ice CorE (TALDICE). The most recent samples (n = 3) are from the last interglacial (Holocene) ice, while the other samples correspond to the Antarctic Cold Reversal (n = 1) and the Last Glacial Maximum (n = 2). These samples include time periods where the environmental factors influencing the sources varied substantially, and therefore represent a suite of possibilities for DOM species and concentrations in polar ice cores.

2. Experimental section

2.1. TALDICE ice core and sample preparation

Talos Dome is located in the Ross Sea sector of East Antarctica, approximately 250 km from the Southern Ocean, 1100 km east of EPICA-Dome C and 550 km north of Taylor Dome. The TALDICE ice core drilling site (159°11′E 72°49′S; 2315 m a.s.l.) is situated near Dome Summit1 and is characterized by an annual mean temperature of −41 °C and a snow accumulation rate of 80 mm water equivalent per year (average 2004–1259 Common Era) (Stenni et al., 2011). This site is sensitive to marine air masses intruding onto the Antarctic Plateau (Spolaor et al., 2013) and moisture sources are mainly from the Pacific and Indian sectors of Southern Ocean (Stenni et al., 2011). The TALDICE ice core is 1620 m deep and spans the last 215 thousand years (kyr). The ice core sample ages were obtained using the AICC2012 age scale (Bazin et al., 2013; Veres et al., 2013).

We analyzed six TALDICE ice core samples that were stored at Ca' Foscari University of Venice at −20 °C until analysis (Table 1). We selected the TALDICE samples in order to investigate the transition between the Last Glacial Maximum and the Holocene. TALDICE 27, TALDICE 52, and TALDICE 606 encompass the Holocene and correspond to ~100, ~300 and ~10,000 yr before present (BP), respectively. TALDICE 726 coincides with the Antarctic Cold Reversal (~13,000 yr BP). The final two samples, TALDICE 1001 and TALDICE 1077, correspond to the glacial period and date back to ~35,000 and ~40,000 yr BP, respectively (Table 1).

Ice core decontamination was performed using a consolidated sample preparation procedure. To eliminate possible trace impurities from the outer layers of the ice core, samples were decontaminated by removing the outermost sample sections with a scalpel under a ISO 6 laminar flow bench in a −20 °C cold room. Each subsequent phase of sample preparation was performed inside an ISO 5 clean room. Ice samples were melted at room temperature in 125 mL LDPE bottles that were previously cleaned by soaking in 5% and 1% HNO_3 solutions for two days. All 1.5 mL glass vials, caps and pipette tips were washed using HPLC/MS-grade methanol and dried under an ISO 5 laminar flow hood. The samples were prepared by transferring 675 μL of melted, decontaminated ice to 1.5 mL glass vials and adding 25 μL of an isotopically-labeled $^{13}C_6$ vanillin (VAN*) solution with a concentration of 5.6 ng μL^{-1} VAN* in ultrapure water resulting in a final internal standard concentration of 200 pg μL^{-1}. Samples were stored at −20 °C in triple polyethylene bags until the analysis in order to minimize any possible contamination of the samples.

2.2. Instrumental analysis, data processing and molecular assignment

Samples were analyzed using a nano-UPLC-nano-ESI-HRMS technique where a UHPLC Ultimate 3000 (ThermoFisher Scientific, Germany) equipped with a nano pump and an autosampler was coupled to an LTQ Orbitrap XL (ThermoFisher Scientific, Germany).

Table1
Studied Talos Dome ice core samples.

Sample	Top Depth (m)	TD bag AICC2012 Age (yr BP 1950)	Period	Accumulation (1000 kg m^{-2} y^{-1})
TALDICE27	26	103	interglacial	0.0817
TALDICE 52	52	319	interglacial	0.0760
TALDICE 606	605	10,102	interglacial	0.0388
TALDICE 726	725	13,308	Antarctic Cold Reversal	0.0252
TALDICE 1001	1000	34,607	glacial	0.0099
TALDICE 1077	1076	40,294	glacial	0.0130

The ionization was obtained using a Nanospray Flex ion source (ThermoFisher Scientific, Germany) equipped with a Picotip silica emitter (FS 360 μm OD-50 μm ID −15 μm distal ending coating). Four μL of each sample were injected on a HPLC Hypersil Gold IntegraFrit AQ C18 (150 mm × I.D. 75 μm, 1.9 μm) column. Eluent A was 0.01% of formic acid in ultrapure water. All ultra-pure water was produced by a Purelab Chorus 1 system and filtered through a LC pack polisher cartridge (Millipore, Molsheim, France), and a PTFE 0.2 μm filter (Phenomenex). Eluent B was 0.01% of formic acid in acetonitrile (0.2 μm filtered). Elution was performed at a flow rate of 250 nL min^{-1}. Chromatographic conditions were the following: 0–5 min 1% of A, from 5 to 15 min from 1% of A to 99% of B, from 15 to 35 min 99% of B, at 35.1 min 1% of A and isocratic equilibration until 50 min. A typical chromatogram reporting the total ion current is reported in Figure S1. Connections between components utilized nanoViper peek-coated fused silica capillary (1/16″ OD, 20 μm ID) or fused silica capillaries (360 μm, 20 μm ID), using zero dead volume PEEK two pieces micro tight connectors and inline micro filters (0.5 μm) (Upchurch Scientific, IDEX Health and Science) in order to avoid column clogging. Details on injection and mass spectrometer parameters are reported in Table S1. Nano-ESI ionization was performed in negative polarity using a voltage of −2 kV. A post column infusion of methanol at a flow of 100 nL min^{-1} using an integrated syringe pump in LTQ Orbitrap XL stabilized the ionization at the beginning of the chromatographic run. HRMS acquisition was in full scan in a 100–600 m/z mass range at a resolution of 60,000 at m/z 400. Both ultrapure laboratory water as well as ultrapure water purchased directly from vendors often contain more elements and compounds than 4 μL of deep ice core samples. Therefore, the standard methods for creating procedural and laboratory blanks do not apply. Our blanks consisted of void injections: during analysis the autosampler does not inject a sample, it only rotates the injection valve in order to start the HPLC run and the acquisition of data from the mass spectrometer. This procedure is performed in order to test any possible contribution from the combination of the solvents, column, HPLC and Orbitrap.

Mass spectrometer calibration was performed every 48 h using sodium dodecil sulfate, sodium taurocolate, MRFA and Ultramark 1621 (Pierce LTQ ESI Negative Ion Calibration Solution, Thermo Scientific). In order to ensure mass accuracy lower than 2 ppm, lock masses of oleic acid ($[M-H]^{-1}$ m/z 281.2486, stearic acid m/z 283.2643 and palmitic acid m/z 255.2330 were employed during data acquisition (Sleighter et al., 2008). The following analysis of chromatograms highlighted the absence of oleic and stearic acid, while the height of chromatographic peaks of palmitic acid in samples did not significantly differ from those in void injections.

The samples were also analyzed by nano-UPLC-HRMS using the data dependent acquisition consisting of the simultaneous acquisition of HRMS, MS/MS and MS^n. The fragmentation of the precursor ions is acquired at a resolution of 30,000 for the first and the second most intense ions observed during the full scan profiling in the selected mass range. The fragmentation pattern was compared to databases such as Metlin (Metlin) and massBank (MassBank), or with available literature, in order to obtain the tentative identification of compounds (Salek et al., 2013).

Each ice sample was injected three times and data were compared with void injections (blanks) using Sieve 2.0 software (Thermo Scientific) where the detection algorithm was limited to small molecules. Comparing the ice samples versus the blanks as a control group and applying a threshold of 8000 cps for a maximum of 5000 ions, the software calculated a ratio and p-value for each ion detected. The Sieve software was able to distinguish between ions of the same isotopic cluster, where we only considered monoisotopic (^{12}C) ions with intensities greater than five times of the blank values (ratio > 5). Molecular assignments were performed using Xcalibur 2.1.0 software (Thermo Scientific) using guidelines of $^{12}C \leq 100$, $^{1}H \leq 200$, $^{14}N \leq 5$, $^{16}O \leq 50$, $^{32}S \leq 2$. The obtained molecular formulas were filtered using the elemental ratio H/C 0.2–3.1, O/C 0–1.2, N/C 0–1.3, S/C 0–0.8 (Kind and Fiehn, 2007) in order to eliminate formulae not likely present among natural compounds, and discarding formulae with double bond equivalent (DBE), that do not result in integers or numbers > 0 (Wozniak et al., 2008). For example, DBE indicates the number of double bonds and rings where a formula $C_cH_hN_nO_oS_s$, is calculated as (2c + 2-h + n)/2, and results in a whole number ≥ 0 (McLafferty and Turecek, 1993). The majority of the accepted formulas with a mass tolerance of ± 2 ppm agreed with an error mass <1.5 ppm (Table 2). The assigned formulas were checked for the nitrogen rule (Koch et al., 2005), and those containing ^{32}S were checked for possible counterparts containing ^{34}S.

3. Results and discussion

3.1. Nano UPLC-nano ESI HRMS analysis

Nano-HPLC systems have a substantially decreased internal diameter of the chromatographic columns, thereby minimizing the in-column dilution of the injected samples, resulting in increased sensitivity of nano-HPLC compared to more common HPLC systems (Vissers, 1999). Moreover, nano ElectroSpray Ionization (nano-ESI) produces smaller droplets in comparison to conventional ESI sources (Juraschek et al., 1999; Schmidt et al., 2003), improving the efficiency of desolvation, and ionization (Wilm and Mann, 1996). Further advantages deriving from the combination of ESI techniques with liquid chromatography include reducing of ion suppression, as well as improving the separation of isomers and coeluting compounds (De Vos et al., 2007). The nano-ESI technique is also more resistant to salt contamination (Juraschek et al., 1999). In addition, substituting the HPLC with a UPLC improves sensitivity when using a chromatographic column packed with sub-2-μm particles (Churchwell et al., 2005; Yu et al., 2006). In this work we used a Hypersil Gold IntegraFrit AQ C18 (1.9 μm) UPLC column connected to the nano-ESI-HRMS. The resulting coupling of UPLC and HRMS is a valuable technique to investigate complex organic mixtures (Kaufmann, 2014) or for analyzing samples containing low concentrations of organic matter such as ice samples.

In order to check the chromatographic quality and the mass calibration accuracy, VAN* was added to the ice samples to achieve a final concentration of 200 pg μL^{-1}. During sample analyses the

Table 2
Summary of information regarding the number of formulas assigned and metrics determined in overall and in each TALDICE sample.

	CHO						CHON						CHOS						CHONS					
	Number of ions	O/C (min–max)	H/C (min–max)	DBE (min–max)	OSc (mean ± std dev)	Δppm (mean ± std dev)	Number of ions	O/C (min–max)	H/C (min–max)	DBE (min–max)	Δppm (mean ± std dev)		Number of ions	O/C (min–max)	H/C (min–max)	DBE (min–max)	Δppm (mean ± std dev)		Number of ions	O/C (min–max)	H/C (min–max)	DBE (min–max)	Δppm (mean ± std dev)	
27	168	0.1–1.0	0.7–2.2	0–14	−1.0 ± 0.4	0.3 ± 0.7	26	0.1–0.8	0.7–2.1	1–13	0.4 ± 0.7		21	0.1–1.4	0.6–2.2	0–13	0.3 ± 0.8		10	0.1–0.7	1.0–2.1	1–9	0.3 ± 0.8	
52	141	0.1–1.1	0.7–2.2	0–14	−0.9 ± 0.5	0.3 ± 0.7	32	0.2–0.8	0.7–2.1	1–13	0.4 ± 0.6		39	0.1–1.5	0.6–2.1	0–13	0.2 ± 0.8		9	0.1–0.7	1.4–2.1	1–9	0.5 ± 0.9	
606	147	0.1–1.0	0.7–2.2	0–14	−1.0 ± 0.5	0.2 ± 0.8	40	0.1–0.8	0.7–2.1	1–13	0.3 ± 0.8		29	0.1–1.4	0.6–2.2	0–13	0.4 ± 0.8		6	0.1–0.7	1.3–2.1	1–9	0.5 ± 0.9	
726	103	0.1–0.7	0.7–2.2	0–14	−1.1 ± 0.4	0.3 ± 0.7	24	0.2–0.7	0.8–2.1	1–13	0.3 ± 0.9		17	0.1–0.9	0.8–2.2	0–11	0.6 ± 0.5		7	0.1–0.4	0.8–2.1	1–10	0.2 ± 0.8	
1001	75	0.1–0.7	0.6–2.2	0–19	−0.9 ± 0.5	0.3 ± 0.7	8	0.1–0.5	0.7–2.1	1–17	0.5 ± 0.5		27	0.1–1.0	0.9–2.2	0–11	0.3 ± 0.8		4	0.1–0.5	1.4–2.1	1–9	0.4 ± 1.0	
1077	71	0.1–0.7	0.7–2.2	0–14	−1.0 ± 0.5	0.1 ± 0.8	20	0.2–0.5	1.0–2.1	1–13	0.5 ± 0.7		21	0.1–0.9	0.8–2.2	0–11	0.5 ± 0.7		3	0.1–0.4	1.4–2.1	1–9	0.1 ± 1.0	
For all samples						205	0.1–1.1	0.6–2.2	0–19		−0.9 ± 0.4		0.2 ± 0.7	49	0.1–0.8	0.7–2.1	1–17		0.3 ± 0.8	48	0.1–1.5	0.-2.2	0–13	
	0.2 ± 0.8	15	0.1–0.7	0.8–2.1	1–10	0.4 ± 0.8																		

mean error for the mass accuracy of VAN* was 1.1 ± 0.5 ppm. VAN* also helps evaluate the increase in sensitivity of the analytical method using nano-UPLC-nano-ESI-HRMS compared to the direct infusion in nano-ESI-HRMS. Using both techniques, we compared the absolute signal intensities of the ion at m/z 157.0602 ([VAN* - H] $^-$) in sample TALDICE 27, which is the most abundant available TALDICE sample. Instrumental parameters of the mass spectrometer for the nano-ESI-HRMS and nano-UPLC-nano-ESI-HRMS systems were the same in both experiments (Table S1). In order to use the same injection conditions, 250 μL of TALDICE 27 ice sample was diluted with 100 μL methanol + 0.01% formic acid, before the direct injection into the nano-ESI source (flow 350 nL min^{-1}, 3 replicates). For nano-UPLC-nano-ESI-HRMS analysis, 4 μL of the TALDICE 27 ice sample was injected into the column. The flow through the column was 250 nL min^{-1}, where the post-column addition of methanol resulted in a flow of 350 nL min^{-1} entering the nano-ESI. We performed three replicates and examined the ion intensity (cps) of m/z 157.0602 in the mass spectra at the VAN* chromatographic peak. Nano-UPLC-nano-ESI-HRMS analysis showed a mean intensity and a signal to noise ratio (corresponding to the ion m/z = 157.0602) of 1576 and 326 times higher than nano-ESI-HRMS results.

In order to tentatively identify compounds, we compared our results with databases (Metlin (Metlin) and massBank (MassBank)) and the available literature (Niessen and Correa, 2017; Steimer et al., 2017). These identified compounds include fatty acids C_5-C_{26}, some hydroxyl fatty acids: $C_8H_{16}O_3$ (2- or 8-hydroxyoctanoic acid), $C_9H_{18}O_3$ (hydroxynonanoic acid), $C_{10}H_{20}O_3$ (10-hydroxydecanoic acid), $C_{12}H_{24}O_3$ (12-hydroxydodecanoic acid), $C_{16}H_{32}O_3$ (2-hydroxyhexadecanoic acid), $C_5H_8O_3$ (5-oxo-pentanoic acid), $C_6H_{10}O_4$ (adipic acid), $C_8H_{14}O_4$ (suberic acid), $C_9H_{16}O_4$ (azelaic acid), $C_8H_8O_3$ (vanillin), and $C_9H_8O_3$ (coumaric acid). An additional twelve compounds produced fragmentation with losses of CO_2 typical of the carboxylic functional group (Niessen and Correa, 2017; Steimer et al., 2017) that coincide with the chemical formula of oxo fatty acids, dicarboxylic acids and compounds from the photo-oxidation of monoterpene (Table S2). The CHON and CHONS classes did not register fragmentation, while the two precursor ions for the CHOS class, $C_{12}H_{25}O_4S^-$ and $C_{14}H_{29}O_4S^-$, produced the fragment HSO_4^- at m/z 96,9603 that is characteristic of organosulfates (Gomez-Gonzalez et al., 2008).

3.2. Van Krevelin analysis

Molecular characterization of DOM in polar snow and ice generally requires melted sample volumes from 100 to 150 mL (Antony et al., 2014; Antony et al., 2017) to 900 mL (Grannas et al., 2006) in order to detect thousands of molecular species. However, multi-proxy deep ice cores have maximum available sample sizes of only a few milliliters. Although nano system technology increases the signal intensity, the nano-HPLC-nano-ESI-HRMS technique using a limited volume of 4 μL can detect only the major species in ice samples. In our samples, 580 ions were significant compared to blanks (ratio > 5), where we assigned molecular formulas for 317 ions. These ions can be grouped in four subgroups: 205 (65% of the total) formulas contained only CHO atoms, 49 (15%) included formulas with CHON atoms, 48 (15%) CHOS and 15 (5%) CHONS atoms (Table 2). These results agree with Antony et al. (2014), who determined that CHO formulas are the major category of compounds in Antarctic snow. Mazzoleni et al. (Mazzoleni et al., 2012) observed a similar result in non-urban aerosols. Among the 3737 assigned formulas, only 373 species (of which 326 were CHO) had relative abundances >10% (Mazzoleni et al., 2012). Therefore, both atmospheric aerosols and ice cores only contain a few hundred major species. Among the 39 formulas (relative abundances >10%) reported by Mazzoleni et al. (Mazzoleni et al.,

2012), such as $C_9H_{14}O_4$, $C_{10}H_{16}O_5$, $C_{10}H_{16}O_6$, $C_{13}H_{20}O_5$, $C_{14}H_{22}O_5$, $C_{14}H_{22}O_6$ etc fourteen were also found in TALDICE samples.

The aromaticity index (AI) (Koch and Dittmar, 2006; Koch and Dittmar, 2016) classifies molecules based on the number of DBE and only includes molecules that contribute to aromaticity, ring formation or condensation. AI classifies molecules as aliphatic (AI = 0), olefinic ($0 < AI \leq 0.5$), aromatics ($AI > 0.5$) and condensed aromatics ($AI \geq 0.67$). The majority of assigned formulas in this work represent aliphatic compounds (77%); 17% are olefinic, while only 3% are aromatics and 3% are condensed aromatics. This result is consistent with the high number of aliphatic-type (AI = 0) compounds observed in the literature that refer to algal detritus and/or microbial biomass. The scarcity of aromatics and condensed aromatic compounds in our samples (Table 2) is reasonable due to the photolabile nature of these compounds (Stubbins et al., 2010; von Schneidemesser et al., 2012).

Van Krevelin diagrams (Kim et al., 2003) plot atomic ratios of H/C vs O/C where major biomolecular components fall within specific regions of the plot. These plot areas include the following: lipids (O/C 0–0.2, H/C 1.7–2.2), proteins and amino sugars (O/C 0.2–0.6, H/C 1.5–2.2, $N/C \geq 0.05$), carbohydrates (O/C 0.6–1.2, H/C 1.5–2.2), lignin-like compounds (O/C 0.1–0.6, H/C 0.6–1.7, AI < 0.67), tannins (O/C 0.6–1.2, H/C 0.5–1.5, AI < 0.67), unsaturated hydrocarbons (O/C 0–0.1, H/C 0.7–1.5) and condensed aromatics (O/C 0–1, H/C 0.3–0.7, $AI \geq 0.67$) (Antony et al., 2014). Additional research (Wozniak et al., 2008) ascribes the region of $O/C \sim 0.4–0.7$ and $H/C \sim 1.0–1.7$ to atmospheric secondary organic aerosol (SOA). However, not every compound that falls within these Van Krevelin diagram regions belong to these specific biomarker groups (Mazzoleni et al., 2012). In the Van Krevelin diagram of DOM in ice (Fig. 1) the most populated regions are those related to lignins (44%), SOA-like species (14%), lipids (10%), proteins/amino sugars (10%), and carbohydrates (9%).

3.3. Compounds containing CHO atoms

Antarctic ice is a complex matrix containing organic material from multiple sources. Recent analyses of Antarctic surface snow (Antony et al., 2014; Antony et al., 2017) confirm continental sources, as well as primary and secondary organic aerosols from oceanic emissions. Microbial communities also contribute to the organic content by releasing proteins and lipids (Antony et al., 2014; Antony et al., 2017).

In TALDICE samples 24% of assigned formulas were similar to formulas in Antarctic snow (Antony et al., 2014; Antony et al., 2017). Numerous molecular formulas in the deep TALDICE ice core DOM are consistent with fatty acids (Fu et al., 2013) in a shallow ice core from southern Alaska (Pokhrel et al., 2015). In Antarctica, both saturated and unsaturated fatty acids may originate from algal and bacterial communities where these fatty acids exist in the snow pack (Antony et al., 2014; Antony et al., 2017; Lopatina et al., 2013), ice cores (Achberger et al., 2011; Antony et al., 2012) and sea ice (Lizotte, 2001), as well as from marine phytoplankton and bacteria (Fahl and Kattner, 1993; Bottino, 1974). Seawater may be an additional source of fatty acids (Kieber et al., 1997) where freshly-emitted sea spray contains saturated and unsaturated fatty acids, dicarboxylic acids (DCAs), oxo-fatty acids, as well as saturated hydroxy fatty acids (Cochran et al., 2016). Bubbles bursting at the sea surface can also transfer unsaturated fatty acids to the atmosphere where they can be oxidized into mono carboxylic acids, oxo-carboxylic acids, and DCAs (Gallimore et al., 2017; Kawamura and Bikkina, 2016; Reynolds et al., 2006). DCAs in water (Yang et al., 2008) and at the air/water interface can also further degrade into the previously-listed molecules (Enami et al., 2015), where these degradation products can also enter the atmosphere. Longer chain DCAs oxidize to shorter DCAs (Kawamura and Bikkina, 2016) during atmospheric long range transport (LRT). Once these materials are deposited on the ice, DCAs can photo-oxidize in the ice matrix producing shorter DCAs and more oxidized products such as CO_2 (Gao and Abbatt, 2011). Fatty acids produced by terrestrial plants may also reach the Antarctic plateau through long range transport.

All classes of fatty acids and their degradation products (Oxfatty acids) exist in the six TALDICE samples analyzed in this paper (Table S2). This result demonstrates the contribution of primary sources such as algae, bacteria, and of primary and secondary aerosols (SOA) to the chemical composition of DOM. Moreover, the presence of fatty acids and Oxfatty acids agrees with the high number of aliphatic-type compounds observed (AI = 0) in these samples (Schmidt et al., 2009).

Extensive research examines the photo-oxidation of isoprene and monoterpene compounds (IMTs), such as α-pinene and limonene as well as investigating their oxidation products (OxIMTs) in smog chambers (Bateman et al., 2009; Fan and Zhang, 2004; Glasius et al., 2000; Kourtchev et al., 2015; Kundu et al., 2012; Kundu et al., 2017; Nguyen et al., 2010; Putman et al., 2012). Multiple environmental matrixes contain OxIMTs including non-urban aerosols and forests (Kristensen and Glasius, 2011; Mazzoleni et al., 2012; Zhao et al., 2013), fog (LeClair et al., 2012; Mazzoleni et al., 2010), clouds (Zhao et al., 2013), marine aerosols (Hu et al., 2013), surface Antarctic snow and the TALDICE ice core (Table S2). IMTs may originate from terrestrial vegetation (Claeys et al., 2007; Claeys et al., 2004; Feltracco et al., 2018) and/or oceanic emissions (Luo and Yu, 2010) where they and their oxidation products can reach Antarctica through LRT (Hu et al., 2013). OxIMTs in Southern Ocean atmospheric aerosols can significantly impact marine SOA during phytoplankton blooms (Hu et al., 2013) where these compounds are then deposited onto surface snow and are present in shallow ice cores (Pokhrel et al., 2016).

Formulas attributable to both Oxfatty acids and OxIMTs exist in the TALDICE ice core (Figures S2-S4). The chromatographic separation in our analytical method separates isobaric compounds. This aspect is particularly useful for the series $C_nH_{2n-4}O_3$ and $C_nH_{2n-4}O_4$ for which the literature proposes compounds related to Oxfatty acids (originating from phytoplankton and bacteria), as well as for compounds from OxIMTs (Table S2 and references therein). Some examples regarding the separation of isobaric compounds at m/z 171.0665 ($C_8H_{12}O_4$), m/z 169.0872 ($C_9H_{14}O_3$) and m/z 183.1028 ($C_{10}H_{16}O_3$) are reported in Figure S2-S4. The presence of isobaric compounds suggested that both Oxfatty acids and OxIMTs are plausible sources.

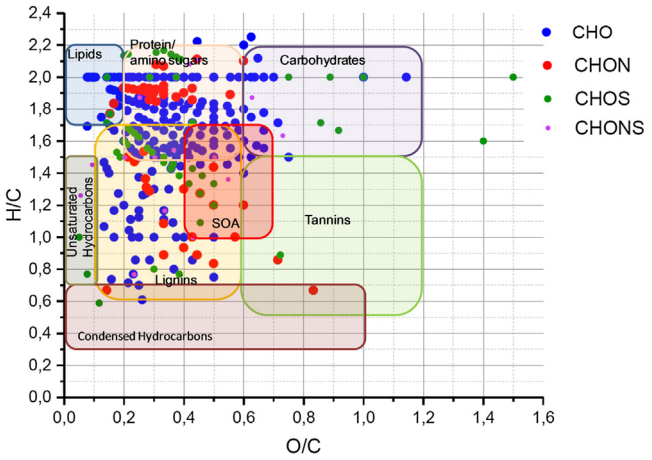

Fig. 1. Van Krevelin plot of all ice core sample molecular formulas detected in negative ion mode.

The ice samples also contain a class of formulas related to carboxylic-rich alicyclic molecules (CRAM) that possibly originate from the ocean. CRAM are refractory materials in marine DOM (Hertkorn et al., 2006) throughout the water column with high concentrations in deep ocean water as well as in lake fresh water (Lam et al., 2007). These compounds may be ejected from the ocean into the atmosphere and reach the Antarctic plateau through atmospheric transport. This group of compounds has the general formula $C_nH_mO_q$ and are defined by the following ratios: DBE/C = 0.30–0.68, DBE/H = 0.20–0.95, DBE/O = 0.77–1.75 (Hertkorn et al., 2006). The TALDICE samples contain 28 compounds, (13.6% of the CHO assigned formulas) that satisfy these ratios.

Further evidence of the contribution of SOA to the organic material in TALDICE ice samples comes from CHO oligomer compounds formed from esterification reactions resulting in a mass increase of $C_3H_4O_2$ (Altieri et al., 2008). We distinguished 40 individual oligomer series composed of two or three compounds differing in mass by 72.0211, which is equivalent to $C_3H_4O_2$. The oligomers accounted for the 24% of the formulas assigned in the CHO subset.

3.4. Compounds containing CHON atoms

Fifty species, including isobaric compounds, were ascribable to the CHON group. The assigned formulas depict H/C 0.7–2.1 and O/C 0.1/08, where DBE ranged between 1 and 17, with a mean value of 4.7 ± 3.4. In the Antarctic ice samples the CHON class contained 1 to 5 nitrogen atoms. Compounds with N_1 represented 35% of total CHON species, while N_2, N_3, N_4 and N_5 were 26%, 4%, 10% and 4% of the total. Subclasses of the assigned formulas include NO_3-NO_6, N_2O_2-N_2O_8, N_3O_4-N_3O_6, and N_4O_3-N_4O_8 that were previously observed in non-urban clouds (Zhao et al., 2013) and in Antarctic snow (Antony et al., 2014). The prominent subclasses are NO_3 and NO_4 representing 44% of compounds. Species with O/N ratio ≥ 3 (Zhao et al., 2013) (functional group $-NO_3$) reached up to 60% of total CHON compounds suggesting a high number of organonitrate species.

Only a few of these formulas had previously been observed in environmental matrices (Table S3). The literature ascribes the following formulas $C_6H_4N_2O_5$, $C_6H_5NO_3$, $C_7H_7NO_3$, and $C_7H_7NO_4$ to dinitrophenol, nitrophenol, methyl nitrophenol, and nitroguaiacol (Kitanovski et al., 2012). All TALDICE samples contained $C_7H_7NO_3$ while the other nitrophenols were only present in TALDICE 27, TALDICE 52, and TALDICE 606. These nitrogen species were also found in atmospheric aerosol (Kitanovski et al., 2012), and nitrophenols were also detected in snow samples from polar regions or high mountains (Matykiewiczova et al., 2007). The presence of these compounds in snow from remote environments may reflect a local atmospheric or snow (photo)chemistry (Matykiewiczova et al., 2007).

3.5. Compounds containing CHOS

The CHOS group contains 49 formulas with H/C 0.6–2.2 and O/C 0.1–1.5 including subclasses from SO to SO_{13}. The $O/S \geq 4$ ratio (Altieri et al., 2009) defines species compatible with the presence of sulfate groups, resulting in a total of 38 out of the 49 compounds (76%), indicating many sulfate compounds among the CHOS species. Organosulfates are tracers of SOAs into the atmosphere produced from the gas phase oxidation of IMTs such as isoprene and α-pinene (Gomez-Gonzalez et al., 2008; Noziere et al., 2010; Surratt et al., 2007) and from oxidation of algal/bacterial unsaturated fatty acid residues (Claeys et al., 2010; Gomez-Gonzalez et al., 2008; Passananti et al., 2016; Shang et al., 2016). Previous studies use organosulfates (sulfate esters) from fatty acids as marine SOA tracers (Fu et al., 2013).

Numerous molecular formulas in the TALDICE ice core coincide with formulas present in Antarctic snow (Antony et al., 2014; Antony et al., 2017) and non-urban clouds (Zhao et al., 2013) (Table S4 and references therein). Our samples include organosulfates from IMT precursors such as isoprene: $C_4H_8O_6S$ (Shalamzari et al., 2013) and $C_5H_8O_7S$ (Altieri et al., 2009) as well as compounds deriving from α-pinene: $C_7H_{12}O_6S$ (Altieri et al., 2009) and $C_{12}H_{26}O_4S$ (Kourtchev et al., 2013). The chromatographic behavior of these compounds is consistent with that reported in the literature (Surratt et al., 2008). Surratt et al. (2008) used a similar reverse phase Acquity HPLC HSS T3 column resulting in compounds deriving from isoprene eluting early in the chromatographic run, and compounds from α-pinene eluting later. In our analysis the retention times for $C_4H_8O_6S$ and $C_5H_8O_7S$ were 6.78 min and 5.06 min, while $C_7H_{12}SO_6$ and $C_{12}H_{26}O_4S$ eluted in a time window of 26.50–30.00 min. The chromatographic analysis demonstrates that three isobaric compounds exist for the formula $C_7H_{12}SO_6$ (ion m/z 223,0284 $C_7H_{11}SO_6^-$; Figure S5). Compounds from isoprene were only present in interglacial samples, while α-pinene existed in all samples. Organosulfates from isoprene had O/C 1.5 and 1.4. These values of organosulfates > 1.2 are consistent with the literature examining the behavior of isoprene in the atmosphere (Altieri et al., 2009; Shalamzari et al., 2013).

3.6. Compounds containing CHONS atoms

The class of CHONS compounds (Table S5) only contains 17 species with varying numbers of N and S. The observed compounds are generally aliphatic (AI = 0) where we attribute a nitrooxy organosulfate ($O \geq 7$) formula (Altieri et al., 2009) to the two isobaric species ($C_{14}H_{21}NSO_7$) (Altieri et al., 2009).

3.7. Differences in CHO compounds in glacial versus interglacial TALDICE ice samples

The largest group of compounds in the TALDICE samples is CHO, which contained a total of 253 (Table S2) species including isobars. In TALDICE 27 we observed 202 CHO species, 156 in TALDICE 52, 160 in TALDICE 606, as well as 115, 79 and 74 in TALDICE 726, TALDICE 1001, and TALDICE 1077, respectively. Among the 253 CHO species, the same 52 compounds were present in every sample where these formulas were only attributable to fatty acids and Oxfatty acids. Only four formulas were ascribable exclusively to OxIMTs (Table S2). The prevalence of these compounds in the TALDICE samples is reasonable as fatty acids and Oxfatty acids compounds can originate in the ocean and subsequently be transported to the ice sheet or they can be produced *in situ* by microorganisms in snow and ice. Excluding the 52 compounds in common the remaining species vary between samples where the interglacial samples encompass more diverse species.

The distribution of OxIMT compounds is substantially different between interglacial and glacial samples. When considering the formulas exclusively attributable to OxIMT the interglacial samples contain a wider variety of OxIMT species than do the glacial samples. The interglacial samples contain the following OxIMT distributions: TALDICE 27 contains 30 different OxIMT species, TALDICE 52 has 23 separate OxIMTs, while TALDICE 606 contains 20 total OxIMT species. However, TALDICE 726 contains 5 OxIMT compounds. The glacial samples TALDICE 1001 and TALDICE 1077 only contain 7 and 4 OxIMTs respectively.

This difference in OxIMTs may be due to temperature changes where cold temperatures during the Last Glacial Maximum (LGM) inhibited terrestrial vegetation growth in the southern high latitudes (Harrison and Goni, 2010) thereby reducing the contribution of OxIMTs through long range transport. Increased sea ice between 16 and 80 ky BP, extended as far as ~500 km north of

the Antarctic coast, (Spolaor et al., 2013) thereby reducing the oceanic sources of IMTs. These factors may also influence TALDICE sample 726 which is from the coldest period of the Antarctic Cold Reversal (Stenni et al., 2011), resulting in a similar distribution of OxIMT species as in the LGM samples.

The fatty acids and Oxfatty acids formulas include saturated fatty acids, hydroxy fatty acids, oxo-fatty acids, DCAs, and unsaturated fatty acids, hydroxy fatty acids, oxo-fatty acids, and DCAs. The number of fatty acids and Oxfatty acids progressively decrease from sample TALDICE 27 to TALDICE 1077. This trend is particularly evident in the unsaturated classes of these compounds, resulting in the following distributions: TALDICE 27 (26 compounds), TALDICE 52 (22), TALDICE 606 (17), TALDICE 726 (12), TALDICE 1001 (12), and TALDICE 1077 (8). The tendency is similar to the decrease in OxIMTS through time and which may also be due to increased sea ice extent during the glacial period. The number of unsaturated compounds also could decrease through time due to oxidation and/or post-depositional reactions (Moise and Rudich, 2002). Snow is a porous medium in which sunlight can penetrate to depths of 10–20 cm to promote photochemical reactions (Domine et al., 2008). Present low accumulation polar regions can contain firn in the top 50 cm of the snow pack that is 10 years old, and therefore has been subject to sunlight for much of this time (Domine et al., 2008). During cold periods, decreased snow accumulation could increase the exposure time of organic compounds (Table 2) thereby decreasing the number of reactive species.

The average carbon oxidation state (OSc) (Kroll et al., 2011) helps determine how complex mixtures of organic compounds respond to dynamic oxidation processes. OSc is calculated using the formula OSc ≈ 2O/C − H/C (Kroll et al., 2011). The Antarctic ice samples have similar chemical compositions with mean OSc values ranging between −0.9 and −1.1 (Table 2). However, combining the OSc values with DBE results helps isolate groups of compounds from fatty acids and IMTs. The mean OSc (-1.5 ± 0.2) and mean DBE (1.2 ± 0.5; ranging between 1 and 3) depicts saturated and unsaturated fatty acids and hydroxy fatty acids. Saturated and unsaturated Oxfatty acids and DCAs encompass mean OSc values of 1.0 ± 0.3 and mean DBE of 2.4 ± 0.5 (range 2–3). OxIMT compounds include an OSc of −0.8 ± 0.2 with a mean DBE of 3.4 ± 1.0 (range 1–6).

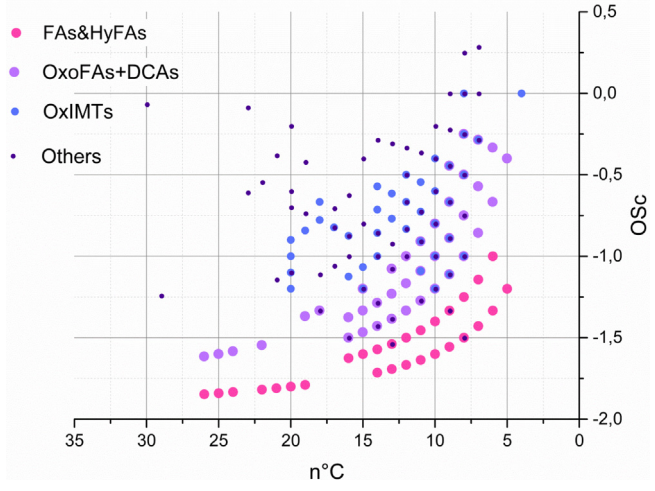

Fig. 2. OSc vs number of carbon atoms in each molecular formula. Pink dots indicate fatty acids and hydroxy fatty acids (FAs&HyFAs), violet dots depict oxo-fatty acids (OxoFAs) and DCAs, light blue circles represent OxMTs, while the dark purple depict the other compounds detected in the TALDICE samples. (For interpretation of the references to colour in this figure legend, the reader is referred to the web version of this article.)

The sample formulas include a heterogeneous group of 95 compounds that to the best of our knowledge is not explained in the literature. This group of compounds contains the most oxidized molecules of the samples (mean OSc of −0.7 ± 0.4) which may represent degradation products from other compounds (Fig. 2). These samples also contain the greatest range in DBE with a mean of 4.6 ± 3.7 (ranging between 0 and 19). Although this final group is heterogeneous, the majority of these compounds are olefinic, where all of the determined aromatic and condensed aromatic compounds fall within this group. Other examples of compounds in this group include $C_8H_8O_3$ and $C_9H_8O_3$ which are tentatively assigned to vanillin and coumaric acid. These compounds originate from lignin (Jex et al., 2014) and were present in the interglacial samples (TALDICE 27, TALDICE 52 and TALDICE 606), which is consistent with the idea of a closer vegetation source during the warmer period.

4. Conclusions

The principal goal of this work is examining if dissolved organic matter in deep ice cores changes over glacial to interglacial timescales. In order to better identify and characterize the compounds, we developed a more sensitive nano-UPLC-nano-ESI-HRMS analytical method that only requires 4 μL of melted ice. We analyzed six samples from the deep TALDICE ice core spanning from the Holocene to the LGM. We detected 580 molecular species and assigned 317 elemental formulas to these compounds. In order to obtain the tentative identification of formulas assigned, when available, we compared the MS/MS fragmentation with those in data banks and the available literature. Comparing formulas attributed to ions detected in this work with formulas obtained from the characterization of specific emission sources and environmental matrixes helps in attributing possible origins for the compounds in TALDICE core. The majority of the identified species are generally aliphatic, encompassing saturated and unsaturated fatty acids, hydroxyl fatty acids and their degradation products, species from the oxidation of isoprene and monoterpenes, as well as a heterogenous group of oxidized compounds. These compounds are consistent with recognized sources contributing to the chemical composition of DOM in polar ice: bacteria and algae in snow and ice, primary and secondary aerosols from marine sources and/or from LRT, and compounds produced *in situ*.

The number of molecular species substantially decreased from the interglacial to the glacial samples, with a reduction in the number of OxIMTs, and where unsaturated fatty acids and Oxfatty acids became almost nonexistent. This decrease in dissolved organic matter in glacial samples may be due to greater distances to the primary emission sources of OxIMTs from increased sea ice extent and/or decreased terrestrial vegetation. The low accumulation during the glacial period may have exposed unsaturated fatty acids and Oxfatty acids, to longer periods in the upper snowpack layers where they could be subject to oxidation reactions. To the best of our knowledge these are the first, though qualitative, indicators of the behavior of OxIMTs, fatty acids and Oxfatty acids over a glacial/interglacial timescale and the first attempt to characterize dissolved organic matter in a deep ice core.

Declaration of Competing Interest

The authors declare that they have no competing interests.

Acknowledgments

This research received financial support from the Early Human Impact ERC Advanced Grant of the European Commission's VII

Framework Program, grant number 267696, by Programma Nazionale di Ricerche in Antartide (PNRA) Grant: PEA 2013/B2.05, and by European Union Marie Curie IIF Fellowship (MIF1-CT-2006-039529, TDICOSO) within the VII Framework Program. The Talos Dome Ice Core Project (TALDICE), a joint European programme, is funded by national contributions from Italy, France, Germany, Switzerland and the United Kingdom. Primary logistical support was provided by PNRA at Talos Dome. The authors gratefully acknowledge the help of ELGA LabWater in providing the Chorus I and Chorus II that produced the ultrapure water used in these experiments. Any use of trade, firm, or product names is for descriptive purposes only and does not imply endorsement by the U.S. Government.

Appendix A. Supplementary data

Supplementary data to this article can be found online at https://doi.org/10.1016/j.scitotenv.2019.134432.

References

Achberger, A.M., Brox, T.I., Skidmore, M.L., Christner, B.C., 2011. Expression and partial characterization of an ice-binding protein from a bacterium isolated at a depth of 3,519 m in the Vostok ice core, Antarctica. Front. Microbiol. 2. https://doi.org/10.3389/fmicb.2011.00255.

Altieri, K.E., Seitzinger, S.P., Carlton, A.G., Turpin, B.J., Klein, G.C., Marshall, A.G., 2008. Oligomers formed through in-cloud methylglyoxal reactions: Chemical composition, properties, and mechanisms investigated by ultra-high resolution FT-ICR mass spectrometry. Atmos. Environ. 42, 1476–1490. https://doi.org/10.1016/j.atmosenv.2007.11.015.

Altieri, K.E., Turpin, B.J., Seitzinger, S.P., 2009. Oligomers, organosulfates, and nitrooxy organosulfates in rainwater identified by ultra-high resolution electrospray ionization FT-ICR mass spectrometry. Atmos. Chem. Phys. 9, 2533–2542. https://doi.org/10.5194/acp-9-2533-2009.

Antony, R., Grannas, A.M., Willoughby, A.S., Sleighter, R.L., Thamban, M., Hatcher, P. G., 2014. Origin and Sources of Dissolved Organic Matter in Snow on the East Antarctic Ice Sheet. Environ. Sci. Technol. 48, 6151–6159. https://doi.org/10.1021/es405246a.

Antony, R., Krishnan, K.P., Laluraj, C.M., Thamban, M., Dhakephalkar, P.K., Engineer, A.S., et al., 2012. Diversity and physiology of culturable bacteria associated with a coastal Antarctic ice core. Microbiol. Res. 167, 372–380. https://doi.org/10.1016/j.micres.2012.03.003.

Antony, R., Willoughby, A.S., Grannas, A.M., Catanzano, V., Sleighter, R.L., Thamban, M., et al., 2017. Molecular Insights on Dissolved Organic Matter Transformation by Supraglacial Microbial Communities. Environ. Sci. Technol. 51, 4328–4337. https://doi.org/10.1021/acs.est.6b05780.

Barbaro, E., Spolaor, A., Karroca, O., Park, K.-T., Martma, T., Isaksson, E., et al., 2017. Free amino acids in the Arctic snow and ice core samples: Potential markers for paleoclimatic studies. Sci. Total Environ. 607, 454–462. https://doi.org/10.1016/j.scitotenv.2017.07.041.

Bateman, A.P., Nizkorodov, S.A., Laskin, J., Laskin, A., 2009. Time-resolved molecular characterization of limonene/ozone aerosol using high-resolution electrospray ionization mass spectrometry. PCCP 11, 7931–7942. https://doi.org/10.1039/b905288g.

Bazin, L., Landais, A., Lemieux-Dudon, B., Kele, H.T.M., Veres, D., Parrenin, F., et al., 2013. An optimized multi-proxy, multi-site Antarctic ice and gas orbital chronology (AICC2012): 120–800 ka. Clim. Past 9, 1715–1731. https://doi.org/10.5194/cp-9-1715-2013.

Bhatia, M.P., Das, S.B., Longnecker, K., Charette, M.A., Kujawinski, E.B., 2010. Molecular characterization of dissolved organic matter associated with the Greenland ice sheet. Geochim. Cosmochim. Acta 74, 3768–3784. https://doi.org/10.1016/j.gca.2010.03.035.

Bottino, N.R., 1974. The fatty acids fo Antarctic Phytoplankton and Euphausiids. Fatty Acid Exchange among Trophic Levels of the Ross Sea. Mar. Biol. 27, 197–204. https://doi.org/10.1007/BF00391944.

Bradley, R.S., 2015. Chapter 5 - Ice Cores. Paleoclimatology (Third Edition). Academic Press, San Diego, pp. 137-194.

Churchwell, M.I., Twaddle, N.C., Meeker, L.R., Doerge, D.R., 2005. Improving LC-MS sensitivity through increases in chromatographic performance: Comparisons of UPLC-ES/MS/MS to HPLC-ES/MS/MS. Journal of Chromatography B-Analytical Technologies in the Biomedical and Life Sciences 825, 134–143. https://doi.org/10.1016/j.jchromb.2005.05.037.

Claeys, M., Szmigielski, R., Kourtchev, I., Van der Veken, P., Vermeylen, R., Maenhaut, W., et al., 2007. Hydroxydicarboxylic acids: Markers for secondary organic aerosol from the photooxidation of alpha-pinene. Environ. Sci. Technol. 41, 1628–1634. https://doi.org/10.1021/es0620181.

Claeys, M., Wang, W., Ion, A.C., Kourtchev, I., Gelencser, A., Maenhaut, W., 2004. Formation of secondary organic aerosols from isoprene and its gas-phase oxidation products through reaction with hydrogen peroxide. Atmos. Environ. 38, 4093–4098. https://doi.org/10.1016/j.atmosenv.2004.06.001.

Claeys, M., Wang, W., Vermeylen, R., Kourtchev, I., Chi, X.G., Farhat, Y., et al., 2010. Chemical characterisation of marine aerosol at Amsterdam Island during the austral summer of 2006–2007. J. Aerosol Sci. 41, 13–22. https://doi.org/10.1016/j.jaerosci.2009.08.003.

Cochran, R.E., Laskina, O., Jayarathne, T., Laskin, A., Laskin, J., Lin, P., et al., 2016. Analysis of Organic Anionic Surfactants in Fine and Coarse Fractions of Freshly Emitted Sea Spray Aerosol. Environ. Sci. Technol. 50, 2477–2486. https://doi.org/10.1021/acs.est.5b04053.

De Vos, R.C.H., Moco, S., Lommen, A., Keurentjes, J.J.B., Bino, R.J., Hall, R.D., 2007. Untargeted large-scale plant metabolomics using liquid chromatography coupled to mass spectrometry. Nat. Protoc. 2, 778–791. https://doi.org/10.1038/nprot.2007.95.

Domine, F., Albert, M., Huthwelker, T., Jacobi, H.W., Kokhanovsky, A.A., Lehning, M., et al., 2008. Snow physics as relevant to snow photochemistry. Atmos. Chem. Phys. 8, 171–208. https://doi.org/10.5194/acp-8-171-2008.

Enami, S., Hoffmann, M.R., Colussi, A.J., 2015. Stepwise Oxidation of Aqueous Dicarboxylic Acids by Gas-Phase OH Radicals. J. Phys. Chem. Lett. 6, 527–534. https://doi.org/10.1021/jz502432j.

Fahl, K., Kattner, G., 1993. Lipid Content and fatty acid composition of algal communities in sea-ice and water from the Weddell Sea (Antarctica). Polar Biol. 13, 405–409. https://doi.org/10.1007/BF01681982.

Fan, J.W., Zhang, R.Y., 2004. Atmospheric Oxidation Mechanism of Isoprene. Environ. Chem. 1, 140–149. https://doi.org/10.1071/EN04045.

Feltracco, M., Barbaro, E., Contini, D., Zangrando, R., Toscano, G., Battistel, D., et al., 2018. Photo-oxidation products of alpha-pinene in coarse, fine and ultrafine aerosol: a new high sensitive HPLC-MS/MS method. Atmos. Environ. 180, 149–155. https://doi.org/10.1016/j.atmosenv.2018.02.052.

Fu, P.Q., Kawamura, K., Chen, J., Charriere, B., Sempere, R., 2013. Organic molecular composition of marine aerosols over the Arctic Ocean in summer: contributions of primary emission and secondary aerosol formation. Biogeosciences 10, 653–667. https://doi.org/10.5194/bg-10-653-2013.

Gallimore, P.J., Griffiths, P.T., Pope, F.D., Reid, J.P., Kalberer, M., 2017. Comprehensive modeling study of ozonolysis of oleic acid aerosol based on real-time, online measurements of aerosol composition. J. Geophys. Res.-Atmos. 122, 4364–4377. https://doi.org/10.1002/2016JD026221.

Gao, S.S., Abbatt, J.P.D., 2011. Kinetics and Mechanism of OH Oxidation of Small Organic Dicarboxylic Acids in Ice: Comparison to Behavior in Aqueous Solution. J. Phys. Chem. A 115, 9977–9986. https://doi.org/10.1021/jp202478w.

Giorio, C., Kehrwald, N., Barbante, C., Kalberer, M., King, A.C.F., Thomas, E.R., et al., 2018. Prospects for reconstructing paleoenvironmental conditions from organic compounds in polar snow and ice. Quat. Sci. Rev. 183, 1–22. https://doi.org/10.1016/j.quascirev.2018.01.007.

Glasius, M., Lahaniati, M., Calogirou, A., Di Bella, D., Jensen, N.R., Hjorth, J., et al., 2000. Carboxylic acids in secondary aerosols from oxidation of cyclic monoterpenes by ozone. Environ. Sci. Technol. 34, 1001–1010. https://doi.org/10.1021/es990445r.

Gomez-Gonzalez, Y., Surratt, J.D., Cuyckens, F., Szmigielski, R., Vermeylen, R., Jaoui, M., et al., 2008. Characterization of organosulfates from the photooxidation of isoprene and unsaturated fatty acids in ambient aerosol using liquid chromatography/(-) electrospray ionization mass spectrometry. J. Mass Spectrom. 43, 371–382. https://doi.org/10.1002/jms.1329.

Grannas, A.M., Hockaday, W.C., Hatcher, P.G., Thompson, L.G., Mosley-Thompson, E., 2006. New revelations on the nature of organic matter in ice cores. J. Geophys. Res.-Atmos., 111 https://doi.org/10.1029/2005JD006251.

Harrison, S.P., Goni, M.F.S., 2010. Global patterns of vegetation response to millennial-scale variability and rapid climate change during the last glacial period. Quat. Sci. Rev. 29, 2957–2980. https://doi.org/10.1016/j.quascirev.2010.07.016.

Hertkorn, N., Benner, R., Frommberger, M., Schmitt-Kopplin, P., Witt, M., Kaiser, K., et al., 2006. Characterization of a major refractory component of marine dissolved organic matter. Geochim. Cosmochim. Acta 70, 2990–3010. https://doi.org/10.1016/j.gca.2006.03.021.

Hu, Q.H., Xie, Z.Q., Wang, X.M., Kang, H., He, Q.F., Zhang, P.F., 2013. Secondary organic aerosols over oceans via oxidation of isoprene and monoterpenes from Arctic to Antarctic. Sci. Rep. 3, 7. https://doi.org/10.1038/srep02280.

Jex, C.N., Pate, G.H., Blyth, A.J., Spencer, R.G.M., Hernes, P.J., Khan, S.J., et al., 2014. Lignin biogeochemistry: from modern processes to Quaternary archives. Quat. Sci. Rev. 87, 46–59. https://doi.org/10.1016/j.quascirev.2013.12.028.

Juraschek, R., Dulcks, T., Karas, M., 1999. Nanoelectrospray - More than just a minimized-flow electrospray ionization source. J. Am. Soc. Mass Spectrom. 10, 300–308. https://doi.org/10.1016/S1044-0305(98)00157-3.

Kaufmann, A., 2014. Combining UHPLC and high-resolution MS: A viable approach for the analysis of complex samples? Trac-Trends Anal. Chem. 63, 113–128. https://doi.org/10.1016/j.trac.2014.06.025.

Kawamura, K., Bikkina, S., 2016. A review of dicarboxylic acids and related compounds in atmospheric aerosols: molecular distributions, sources and transformation. Atmos. Res. 170, 140–160. https://doi.org/10.1016/j.atmosres.2015.11.018.

Kieber, R.J., Hydro, L.H., Seaton, P.J., 1997. Photooxidation of triglycerides and fatty acids in seawater: Implication toward the formation of marine humic substances. Limnol. Oceanogr. 42, 1454–1462. https://doi.org/10.4319/lo.1997.42.6.1454.

Kim, S., Kramer, R.W., Hatcher, P.G., 2003. Graphical method for analysis of ultrahigh-resolution broadband mass spectra of natural organic matter, the van

Krevelen diagram. Anal. Chem. 75, 5336–5344. https://doi.org/10.1021/ac034415p.
Kind, T., Fiehn, O., 2007. Seven Golden Rules for heuristic filtering of molecular formulas obtained by accurate mass spectrometry. Bmc Bioinformatics 8. https://doi.org/10.1186/1471-2105-8-105.
Kitanovski, Z., Grgic, I., Vermeylen, R., Claeys, M., Maenhaut, W., 2012. Liquid chromatography tandem mass spectrometry method for characterization of monoaromatic nitro-compounds in atmospheric particulate matter. J. Chromatogr. A 1268, 35–43. https://doi.org/10.1016/j.chroma.2012.10.021.
Koch, B.P., Dittmar, T., 2006. From mass to structure: an aromaticity index for high-resolution mass data of natural organic matter. Rapid Commun. Mass Spectrom. 20, 926–932. https://doi.org/10.1002/rcm.2386.
Koch, B.P., Dittmar, T., 2016. From mass to structure: an aromaticity index for high-resolution mass data of natural organic matter (vol 20, pg 926, 2006). Rapid Commun. Mass Spectrometry 30 (2016), 250. https://doi.org/10.1002/rcm.7433.
Koch, B.P., Witt, M.R., Engbrodt, R., Dittmar, T., Kattner, G., 2005. Molecular formulae of marine and terrigenous dissolved organic matter detected by electrospray ionization Fourier transform ion cyclotron resonance mass spectrometry. Geochim. Cosmochim. Acta 69, 3299–3308. https://doi.org/10.1016/j.gca.2005.02.027.
Kourtchev, I., Doussin, J.F., Giorio, C., Mahon, B., Wilson, E.M., Maurin, N., et al., 2015. Molecular composition of fresh and aged secondary organic aerosol from a mixture of biogenic volatile compounds: a high-resolution mass spectrometry study. Atmos. Chem. Phys. 15, 5683–5695. https://doi.org/10.5194/acp-15-5683-2015.
Kourtchev, I., Fuller, S., Aalto, J., Ruuskanen, T.M., McLeod, M.W., Maenhaut, W., et al., 2013. Molecular Composition of Boreal Forest Aerosol from Hyytiala, Finland, Using Ultrahigh Resolution Mass Spectrometry. Environ. Sci. Technol. 47, 4069–4079. https://doi.org/10.1021/es3051636.
Kourtchev, I., Fuller, S.J., Giorio, C., Healy, R.M., Wilson, E., O'Connor, I., et al., 2014a. Molecular composition of biogenic secondary organic aerosols using ultrahigh-resolution mass spectrometry: comparing laboratory and field studies. Atmos. Chem. Phys. 14, 2155–2167. https://doi.org/10.5194/acp-14-2155-2014.
Kourtchev, I., Godoi, R.H.M., Connors, S., Levine, J.G., Archibald, A.T., Godoi, A.F.L., et al., 2016. Molecular composition of organic aerosols in central Amazonia: an ultra-high-resolution mass spectrometry study. Atmos. Chem. Phys. 16, 11899–11913. https://doi.org/10.5194/acp-16-11899-2016.
Kourtchev, I., O'Connor, I.P., Giorio, C., Fuller, S.J., Kristensen, K., Maenhaut, W., et al., 2014b. Effects of anthropogenic emissions on the molecular composition of urban organic aerosols: an ultrahigh resolution mass spectrometry study. Atmos. Environ. 89, 525–532. https://doi.org/10.1021/es3051636.
Kristensen, K., Glasius, M., 2011. Organosulfates and oxidation products from biogenic hydrocarbons in fine aerosols from a forest in North West Europe during spring. Atmos. Environ. 45, 4546–4556. https://doi.org/10.1016/j.atmosenv.2011.05.063.
Kroll, J.H., Donahue, N.M., Jimenez, J.L., Kessler, S.H., Canagaratna, M.R., Wilson, K.R., et al., 2011. Carbon oxidation state as a metric for describing the chemistry of atmospheric organic aerosol. Nat. Chem. 3, 133–139. https://doi.org/10.1038/NCHEM.948.
Kundu, S., Fisseha, R., Putman, A.L., Rahn, T.A., Mazzoleni, L.R., 2012. High molecular weight SOA formation during limonene ozonolysis: insights from ultrahigh-resolution FT-ICR mass spectrometry characterization. Atmos. Chem. Phys. 12, 5523–5536. https://doi.org/10.5194/acp-12-5523-2012.
Kundu, S., Fisseha, R., Putman, A.L., Rahn, T.A., Mazzoleni, L.R., 2017. Molecular formula composition of beta-caryophyllene ozonolysis SOA formed in humid and dry conditions. Atmos. Environ. 154, 70–81. https://doi.org/10.1016/j.atmosenv.2016.12.031.
Lam, B., Baer, A., Alaee, M., Lefebvre, B., Moser, A., Williams, A., et al., 2007. Major structural components in freshwater dissolved organic matter. Environ. Sci. Technol. 41, 8240–8247. https://doi.org/10.1021/es0713072.
Laskin, A., Smith, J.S., Laskin, J., 2009. Molecular Characterization of Nitrogen-Containing Organic Compounds in Biomass Burning Aerosols Using High-Resolution Mass Spectrometry. Environ. Sci. Technol. 43, 3764–3771. https://doi.org/10.1021/es803456n.
LeClair, J.P., Collett, J.L., Mazzoleni, L.R., 2012. Fragmentation Analysis of Water-Soluble Atmospheric Organic Matter Using Ultrahigh-Resolution FT-ICR Mass Spectrometry. Environ. Sci. Technol. 46, 4312–4322. https://doi.org/10.1021/es203509b.
Lizotte, M.P., 2001. The contributions of sea ice algae to Antarctic marine primary production. Am. Zool. 41, 57–73. https://doi.org/10.1668/0003-1569(2001)041[0057:TCOSIA]2.0.CO;2.
Lopatina, A., Krylenkov, V., Severinov, K., 2013. Activity and bacterial diversity of snow around Russian Antarctic stations. Res. Microbiol. 164, 949–958. https://doi.org/10.1016/j.resmic.2013.08.005.
Luo, G., Yu, F., 2010. A numerical evaluation of global oceanic emissions of alpha-pinene and isoprene. Atmos. Chem. Phys. 10, 2007–2015. https://doi.org/10.5194/acp-10-2007-2010.
MassBank, http://massbank.eu/MassBank/
Matykiewiczova, N., Kurkova, R., Klanova, J., Klan, P., 2007. Photochemically induced nitration and hydroxylation of organic aromatic compounds in the presence of nitrate or nitrite in ice. J. Photochem. Photobiol. a-Chem. 187, 24–32. https://doi.org/10.1016/j.jphotochem.2006.09.008.
Mazzoleni, L.R., Ehrmann, B.M., Shen, X.H., Marshall, A.G., Collett, J.L., 2010. Water-Soluble Atmospheric Organic Matter in Fog: Exact Masses and Chemical Formula Identification by Ultrahigh-Resolution Fourier Transform Ion Cyclotron Resonance Mass Spectrometry. Environ. Sci. Technol. 44, 3690–3697. https://doi.org/10.1021/es903409k.
Mazzoleni, L.R., Saranjampour, P., Dalbec, M.M., Samburova, V., Hallar, A.G., Zielinska, B., et al., 2012. Identification of water-soluble organic carbon in non-urban aerosols using ultrahigh-resolution FT-ICR mass spectrometry: organic anions. Environ. Chem. 9, 285–297. https://doi.org/10.1071/EN11167.
McLafferty, F.W., Turecek, F., 1993. Interpretation of Mass Spectra. University Science Books, Sausalito, CA.
McNeill, V.F., Grannas, A.M., Abbatt, J.P.D., Ammann, M., Ariya, P., Bartels-Rausch, T., et al., 2012. Organics in environmental ices: sources, chemistry, and impacts. Atmos. Chem. Phys. 12, 9653–9678. https://doi.org/10.5194/acp-12-9653-2012.
Metlin, M. https://metlin.scripps.edu/landing_page.php?pgcontent=mainPage
Minor, E.C., Steinbring, C.J., Longnecker, K., Kujawinski, E.B., 2012. Characterization of dissolved organic matter in Lake Superior and its watershed using ultrahigh resolution mass spectrometry. Org. Geochem. 43, 1–11. https://doi.org/10.1016/j.orggeochem.2011.11.007.
Moise, T., Rudich, Y., 2002. Reactive uptake of ozone by aerosol-associated unsaturated fatty acids: kinetics, mechanism, and products. J. Phys. Chem. A 106, 6469–6476. https://doi.org/10.1021/jp025597e.
Nguyen, T.B., Bateman, A.P., Bones, D.L., Nizkorodov, S.A., Laskin, J., Laskin, A., 2010. High-resolution mass spectrometry analysis of secondary organic aerosol generated by ozonolysis of isoprene. Atmos. Environ. 44, 1032–1042. https://doi.org/10.1016/j.atmosenv.2009.12.019.
Niessen, W. M. A.; Correa C., R. A., 2017. Interpretation of MS-MS mass spectra of drugs and pesticides. Hoboken, New Jersey: John Wiley & Sons.
Noziere, B., Ekstrom, S., Alsberg, T., Holmstrom, S., 2010. Radical-initiated formation of organosulfates and surfactants in atmospheric aerosols. Geophys. Res. Lett. 37. https://doi.org/10.1029/2009GL041683.
Passananti, M., Kong, L.D., Shang, J., Dupart, Y., Perrier, S., Chen, J.M., et al., 2016. Organosulfate Formation through the Heterogeneous Reaction of Sulfur Dioxide with Unsaturated Fatty Acids and Long-Chain Alkenes. Angewandte Chemie-International Edition 55, 10336–10339. https://doi.org/10.1002/anie.201605266.
Pokhrel, A., Kawamura, K., Ono, K., Seki, O., Fu, P.Q., Matoba, S., et al., 2016. Ice core records of monoterpene- and isoprene-SOA tracers from Aurora Peak in Alaska since 1660s: implication for climate change variability in the North Pacific Rim. Atmos. Environ. 130, 105–112. https://doi.org/10.1016/j.atmosenv.2015.09.063.
Pokhrel, A., Kawamura, K., Seki, O., Matoba, S., Shiraiwa, T., 2015. Ice core profiles of saturated fatty acids (C-12:0-C-30:0) and oleic acid (C-18:1) from southern Alaska since 1734 AD: a link to climate change in the Northern Hemisphere. Atmos. Environ. 100, 202–209. https://doi.org/10.1016/j.atmosenv.2014.11.007.
Putman, A.L., Offenberg, J.H., Fisseha, R., Kundu, S., Rahn, T.A., Mazzoleni, L.R., 2012. Ultrahigh-resolution FT-ICR mass spectrometry characterization of alpha-pinene ozonolysis SOA. Atmos. Environ. 46, 164–172. https://doi.org/10.1016/j.atmosenv.2011.10.003.
Reynolds, J.C., Last, D.J., McGillen, M., Nijs, A., Horn, A.B., Percival, C., et al., 2006. Structural analysis of oligomeric molecules formed from the reaction products of oleic acid ozonolysis. Environ. Sci. Technol. 40, 6674–6681. https://doi.org/10.1021/es060942p.
Salek, R.M., Steinbeck, C., Viant, M.R., Goodacre, R., Dunn, W.B., 2013. The role of reporting standards for metabolite annotation and identification in metabolomic studies. GigaScience 2. https://doi.org/10.1186/2047-217X-2-13.
Schmidt, A., Karas, M., Dulcks, T., 2003. Effect of different solution flow rates on analyte ion signals in nano-ESI MS, or: When does ESI turn into nano-ESI? J. Am. Soc. Mass Spectrom. 14, 492–500. https://doi.org/10.1016/S1044-0305(03)00128-4.
Schmidt, F., Elvert, M., Koch, B.P., Witt, M., Hinrichs, K.U., 2009. Molecular characterization of dissolved organic matter in pore water of continental shelf sediments. Geochim. Cosmochim. Acta 73, 3337–3358. https://doi.org/10.1016/j.gca.2009.03.008.
Schmitt-Kopplin, P., Liger-Belair, G., Koch, B.P., Flerus, R., Kattner, G., Harir, M., et al., 2012. Dissolved organic matter in sea spray: a transfer study from marine surface water to aerosols. Biogeosciences 9, 1571–1582. https://doi.org/10.5194/bg-9-1571-2012.
Shalamzari, M.S., Ryabtsova, O., Kahnt, A., Vermeylen, R., Herent, M.F., Quetin-Leclercq, J., et al., 2013. Mass spectrometric characterization of organosulfates related to secondary organic aerosol from isoprene. Rapid Commun. Mass Spectrom. 27, 784–794. https://doi.org/10.1002/rcm.6511.
Shang, J., Passananti, M., Dupart, Y., Ciuraru, R., Tinel, L., Rossignol, S., et al., 2016. SO2 Uptake on Oleic Acid: A New Formation Pathway of Organosulfur Compounds in the Atmosphere. Environ. Sci. Technol. Lett. 3, 67–72. https://doi.org/10.1021/acs.estlett.6b00006.
Shen, Y.F., Zhao, R., Berger, S.J., Anderson, G.A., Rodriguez, N., Smith, R.D., 2002. High-efficiency nanoscale liquid chromatography coupled on-line with mass spectrometry using nanoelectrospray ionization for proteomics. Anal. Chem. 74, 4235–4249. https://doi.org/10.1021/ac0202280.
Sleighter, R.L., McKee, G.A., Liu, Z., Hatcher, P.G., 2008. Naturally present fatty acids as internal calibrants for Fourier transform mass spectra of dissolved organic matter. Limnol. Oceanogr.-Methods 6, 246–253. https://doi.org/10.4319/lom.2008.6.246.
Smith, J.S., Laskin, A., Laskin, J., 2009. Molecular Characterization of Biomass Burning Aerosols Using High-Resolution Mass Spectrometry. Anal. Chem. 81, 1512–1521. https://doi.org/10.1021/ac8020664.
Spolaor, A., Vallelonga, P., Plane, J.M.C., Kehrwald, N., Gabrieli, J., Varin, C., et al., 2013. Halogen species record Antarctic sea ice extent over glacial-interglacial

periods. Atmos. Chem. Phys. 13, 6623–6635. https://doi.org/10.5194/acp-13-6623-2013.
Steimer, S.S., Kourtchev, I., Kalberer, M., 2017. Mass Spectrometry Characterization of Peroxycarboxylic Acids as Proxies for Reactive Oxygen Species and Highly Oxygenated Molecules in Atmospheric Aerosols. Anal. Chem. 89, 2873–2879. https://doi.org/10.1021/acs.analchem.6b04127.
Stenni, B., Buiron, D., Frezzotti, M., Albani, S., Barbante, C., Bard, E., et al., 2011. Expression of the bipolar see-saw in Antarctic climate records during the last deglaciation. Nat. Geosci. 4, 46–49. https://doi.org/10.1038/NGEO1026.
Stubbins, A., Spencer, R.G.M., Chen, H.M., Hatcher, P.G., Mopper, K., Hernes, P.J., et al., 2010. Illuminated darkness: Molecular signatures of Congo River dissolved organic matter and its photochemical alteration as revealed by ultrahigh precision mass spectrometry. Limnol. Oceanogr. 55, 1467–1477. https://doi.org/10.4319/lo.2010.55.4.1467.
Surratt, J.D., Gomez-Gonzalez, Y., Chan, A.W.H., Vermeylen, R., Shahgholi, M., Kleindienst, T.E., et al., 2008. Organosulfate formation in biogenic secondary organic aerosol. J. Phys. Chem. A 112, 8345–8378. https://doi.org/10.1021/jp802310p.
Surratt, J.D., Kroll, J.H., Kleindienst, T.E., Edney, E.O., Claeys, M., Sorooshian, A., et al., 2007. Evidence for organosulfates in secondary organic aerosol. Environ. Sci. Technol. 41, 517–527. https://doi.org/10.1021/es062081q.
Veres, D., Bazin, L., Landais, A., Kele, H.T.M., Lemieux-Dudon, B., Parrenin, F., et al., 2013. The Antarctic ice core chronology (AICC2012): an optimized multi-parameter and multi-site dating approach for the last 120 thousand years. Clim. Past 9, 1733–1748. https://doi.org/10.5194/cp-9-1733-2013.
Vissers, J.P.C., 1999. Recent developments in microcolumn liquid chromatography. J. Chromatogr. A 856, 117–143. https://doi.org/10.1016/S0021-9673(99)00692-5.
von Schneidemesser, E., Schauer, J.J., Shafer, M.M., Bergin, M.H., 2012. Measurement of loss rates of organic compounds in snow using in situ experiments and isotopically labelled compounds. Polar Res. 31, 1–10. https://doi.org/10.3402/polar.v31i0.11597.
Wilm, M., Mann, M., 1996. Analytical properties of the nanoelectrospray ion source. Anal. Chem. 68, 1–8. https://doi.org/10.1021/ac9509519.
Wolff, E.W., Barbante, C., Becagli, S., Bigler, M., Boutron, C.F., Castellano, E., et al., 2010. Changes in environment over the last 800,000 years from chemical analysis of the EPICA Dome C ice core. Quat. Sci. Rev. 29, 285–295. https://doi.org/10.1016/j.quascirev.2009.06.013.
Wozniak, A.S., Bauer, J.E., Sleighter, R.L., Dickhut, R.M., Hatcher, P.G., 2008. Technical Note: Molecular characterization of aerosol-derived water soluble organic carbon using ultrahigh resolution electrospray ionization Fourier transform ion cyclotron resonance mass spectrometry. Atmos. Chem. Phys. 8, 5099–5111. https://doi.org/10.5194/acp-8-5099-2008.
Yang, L.M., Ray, M.B., Yu, L.E., 2008. Photooxidation of dicarboxylic acids- Part II: Kinetics, intermediates and field observations. Atmos. Environ. 42, 868–880. https://doi.org/10.1016/j.atmosenv.2007.10.030.
Yu, K., Little, D., Plumb, R., Smith, B., 2006. High-throughput quantification for a drug mixture in rat plasma - a comparison of Ultra Performance(TM) liquid chromatography/tandem mass spectrometry with high-performance liquid chromatography/tandem mass spectrometry. Rapid Commun. Mass Spectrom. 20, 544–552. https://doi.org/10.1002/rcm.2336.
Zhao, Y., Hallar, A.G., Mazzoleni, L.R., 2013. Atmospheric organic matter in clouds: exact masses and molecular formula identification using ultrahigh-resolution FT-ICR mass spectrometry. Atmos. Chem. Phys. 13, 12343–12362. https://doi.org/10.5194/acp-13-12343-2013.